Location, Orientation and Aggregation of Bardoxolone-ME, CDDO-ME, in a Complex Phospholipid Bilayer Membrane

Vicente Galiano[1] · José A. Encinar[2,3] · José Villalaín[2,3]

Abstract

Bardoxolone methyl (CDDO-Me), a synthetic derivative of the naturally occurring triterpenoid oleanolic acid, displays strong antioxidant, anticancer and anti-inflammatory activities, according to different bibliographical sources. However, the understanding of its molecular mechanism is missing. Furthermore, CDDO-Me has displayed a significant cytotoxicity against various types of cancer cells. CDDO-Me has a noticeable hydrophobic character and several of its effects could be attributed to its ability to be incorporated inside the biological membrane and therefore modify its structure and specifically interact with its components. In this study, we have used full-atom molecular dynamics to determine the location, orientation and interactions of CDDO-Me in phospholipid model membranes. Our results support the location of CDDO-Me in the middle of the membrane, it specifically orients so that the cyano group lean towards the phospholipid interface and it specifically interacts with particular phospholipids. Significantly, in the membrane the CDDO-Me molecules specifically interact with POPE and POPS. Moreover, CDDO-Me does not aggregates in the membrane but it forms a complex conglomerate in solution. The formation of a complex aggregate in solution might hamper its biological activity and therefore it should be taken into account when intended to be used in clinical assays. This work should aid in the development of these molecules opening new avenues for future therapeutic developments.

Keywords Bardoxolone methyl · CDDO-me · Molecular dynamics · Membrane location

Introduction

Triterpenoids are biosynthesised by many different plants, they are very profuse in leaves, fruits and seeds, and they have been used in traditional medicine in many Asian countries. They comprise a large family of structurally related biomolecules, the cyclosqualenoids, possessing unique biological properties and widely distributed in nature (Dzubak et al. 2006; Itokawa et al. 2008). This surplus of pharmacological beneficial properties include antiviral, antidiabetic, antimicrobial, anti-inflammatory, antioxidant, antitumor, antiparasitic and hepatoprotective effects, cardio- and neuroprotective roles as well as regulation of glucose homeostasis (Peron et al. 2018; Sheng and Sun 2011).

Several analogues have been synthesized in order to increase the biological properties of the parent compounds. One of them is bardoxolone methyl (CDDO-Me, Fig. 1a), a synthetic derivative of the naturally occurring triterpenoid oleanolic acid, which displays potent antioxidant, anticancer and anti-inflammatory activities (Liby and Sporn 2012; Mathis and Cui 2016; Shanmugam et al. 2014). CDDO-Me

✉ José Villalaín
jvillalain@umh.es

1 Physics and Computer Architecture Department, Desarrollo e Innovación en Biotecnología Sanitaria (IDiBE), Universitas "Miguel Hernández", 03202 Elche-Alicante, Spain

2 Instituto de Biología Molecular y Celular (IBMC), Desarrollo e Innovación en Biotecnología Sanitaria (IDiBE), Universitas "Miguel Hernández", 03202 Elche-Alicante, Spain

3 Instituto de Investigación, Desarrollo e Innovación en Biotecnología Sanitaria (IDiBE), Universitas "Miguel Hernández", 03202 Elche-Alicante, Spain
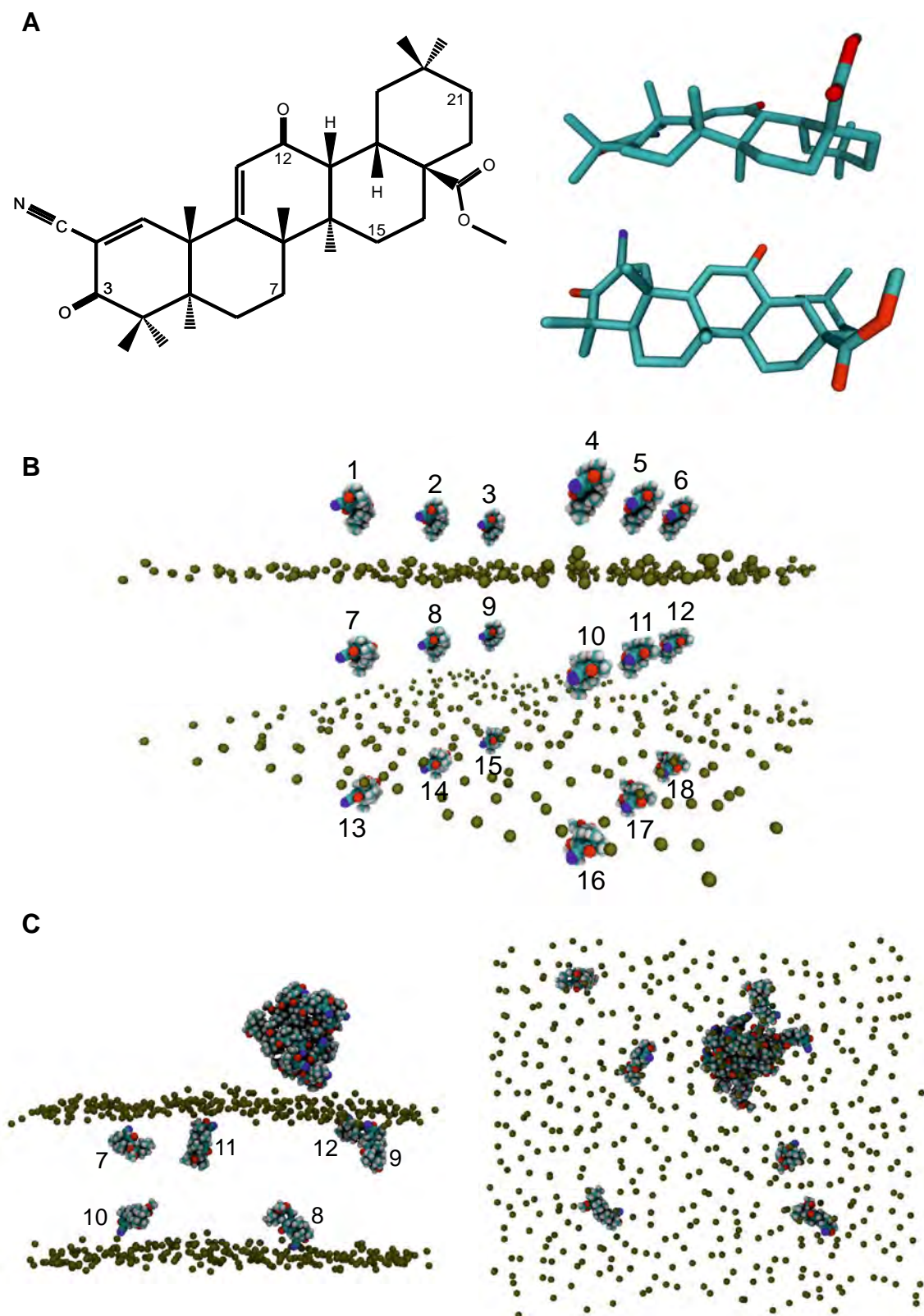
◀**Fig. 1 a** Chemical and molecular structures of the pentacyclic triterpenoid bardoxolone methyl (CDDO-Me, 2-cyano-3,12-dioxo-oleana-1,9(11)-dien-28-oic acid methyl ester). Numbering of particular atoms mentioned in the text is also given. Hydrogens have been omitted for clarity. **b** Initial disposition of the eighteen (numbered) CDDO-Me molecules in the model membrane system. The CDDO-Me molecules and the phosphate atoms of the phospholipids, which define the upper and lower boundaries of the membrane, are shown in VDW representation. **c** Final ($t = 325$ ns) snapshot of the membrane model system POPC/POPE/POPS/PSM/CHOL containing the 18 CDDO-Me molecules. The side and top views are shown. Both the CDDO-Me molecules and phospholipid phosphate atoms (drawn in tan color) are shown in VDW drawing style. The phosphate atoms clearly define the boundary between the exterior and interior part of the membrane. The lipid, sodium and water molecules have been removed for clarity. The numbering of the CDDO-Me molecules inside the membrane are shown

is a bioactive compound and a member of triterpenoid cyanoacrylates, which has displayed a promising activity for prevention and treatment of cancer, exhibiting a significant cytotoxicity against various types of cancer cells (Wang et al. 2014) and inducing tumour regression in different preclinical studies (Deeb et al. 2009; Gao et al. 2015; Mathis and Cui 2016). CDDO-Me has been also evaluated in phase I clinical trials showing relatively good tolerance (Hong et al. 2012; Mathis and Cui 2016). CDDO-Me has been also used in diabetes, pulmonary arterial hypertension, mitochondrial myopathies as well as chronic kidney disease and different clinical trials are currently ongoing (Huang et al. 2017) in spite of having been proven that CDDO-Me can produce serious cardiovascular side effects in sensitive patients (Zeeuw et al. 2013). These effects have been ascribed to the inhibition of nuclear factor kappaB and modulation of the endothelin pathway (Chin et al. 2014). CDDO-Me is also capable of inducing apoptosis, promotion of autophagy and triggering endoplasmic reticulum stress (Wang et al. 2017). Moreover, it down-regulates the expression of the Na^+, K^+-ATPase α1 (Wang et al. 2017). It has been described that CDDO-Me might induce the depletion of mitochondrial glutathione as well as the impairing of the mitochondrial energy supply and be, at least in part, responsible for its cytotoxic effects (Refaat et al. 2017; Samudio et al. 2008). CDDO-Me side effects could be attributable to the modification of different thiol groups of biomolecules, specifically proteins, through its highly reactive α-cyano-α,β-unsaturated ketone group, since CDDO-Me has been proven to interact with many types of proteins (Huang et al. 2017; Yore et al. 2011). CDDO-Me is therefore a promising candidate for cancer treatment. Many signalling pathways have been implicated in the biological effects of CDDO-Me (Liby and Sporn 2012), but the mechanisms of the anticancer effects of CDDO-Me are unknown.

The chemical name of CDDO-Me is 2-cyano-3,12-dioxo-oleana-1,9(11)-dien-28-oic acid methyl ester (Fig. 1a). Due to its highly hydrophobic character and its

great phospholipid/water partition coefficient (XlogP3 value 6.72, https://pubchem.ncbi.nlm.nih.gov/compound/Bardoxolone-methyl#section=Chemical-and-Physical-Properties), CDDO-Me possible effects on biological systems could be attributed to its ability to reside in the biological membrane, modify its fluidity, morphology and permeability as well as specifically interact with its lipid components (Samudio et al. 2006). Moreover, the clinical use of CDDO-Me could be hampered by its relatively low solubilisation in water, phenomenon which could be dependent on the concentration and the buffer used. For example, polyethyleneglycol have been used for making CDDO-Me stock solutions suggesting that CDDO-Me might be not completely soluble in water (Jin et al. 2017). It is important to note that the lipophilicity of a molecule can be assessed from its partition coefficient but it does not give any evidence about its location and orientation in the membrane. Moreover, the interaction of the CDDO-Me molecule with phospholipids and its membrane location might change the membrane physical properties and therefore modulate its interaction with other biological molecules, especially with membrane proteins, what could explain its biological activities (Zalba and Hagen 2017). CDDO-Me biological effects could also depend on both its orientation and location at the membrane, as well as the possible interactions it might have with specific membrane phospholipids. Depending on these factors, CDDO-Me could be oriented at two different dispositions in the membrane, either perpendicular or parallel to the membrane surface, which could exert a significant geometrical deformation on lipid arrangement. Therefore, CDDO-Me could act through hydrophobic interactions with the cell membrane, as well as through interaction with cellular proteins. The knowledge of the CDDO-Me mechanism of action might reveal new avenues for upcoming therapeutic developments, especially considering the evolution of this compound to improve its activity and reduce its side effects.

In this work we have used full-atom molecular dynamics (MD) to discern first, the location and orientation of CDDO-Me in a complex model membrane, and second, the existence of specific interactions with membrane lipids. Therefore, we have used a model membrane composed of the phospholipids 1-palmitoyl-2-oleoyl-*sn*-glycero-3-phosphocholine (POPC), 1-palmitoyl-2-oleoyl-*sn*-glycero-3-phosphoethanolamine (POPE), 1-palmitoyl-2-oleoyl-*sn*-glycero-3-phosphoserine (POPS), and *N*-palmitoyl-D-erythro-sphingosyl-phosphorylcholine (PSM), as well as cholesterol (Chol). Our data support the location of the CDDO-Me molecules in the membrane as well as they specifically orient so that the cyano group tend in the direction of the phospholipid interface. We describe various specific interactions of CDDO-Me with certain lipids of the membrane and its aggregation in

aqueous solution. All these facts could explain, at least in part, some of the interesting biological effects that possess the CDDO-Me molecule.

Experimental Section

Molecular Dynamics Simulation

Unrestrained all-atom molecular dynamics simulations were carried out using NAMD 2.12 (Phillips et al. 2005) with the CHARMM36 force field for the protein (Best et al. 2012) and the CHARMM general force field for the CDDO-Me molecule (Vanommeslaeghe et al. 2010). The TIP3P model was used for water (Jorgensen et al. 1983). All simulations were carried out with a constant number of particles as an NPT ensemble at 1.0 atm and 310 K. The time step was 1 fs. Constant pressure was maintained by the Nosé-Hoover Langevin piston method (Feller 1995; Martyna 1994). Constant temperature was maintained by Langevin dynamics with a damping coefficient γ of 0.5 ps-1. The standard PME method was used with periodic boundary conditions to calculate the long-range electrostatic interaction of the systems. Non-bonded interactions were cut off after 12 Å with a smoothing function applied after 10 Å (Patra et al. 2003). In order to remove overlaps and unfavourable atomic contacts, prior to simulation a minimization for 50,000 steps and an equilibration for 1 ns was made. The production trajectory was calculated for 325 ns.

Bilayer Membrane Model

We have used a lipid bilayer model representing a generic membrane model mixture which was composed of a total of 560 lipid molecules in a rectangular box. Each leaflet contained 120 molecules of 1-palmitoyl-2-oleoyl-*sn*-glycero-3-phosphocholine (POPC), 40 molecules of 1-palmitoyl-2-oleoyl-*sn*-glycero-3-phosphoethanolamine (POPE), 40 molecules of 1-palmitoyl-2-oleoyl-*sn*-glycero-3-phosphoserine (POPS), 40 molecules of *N*-palmitoyl-sphingomyelin (PSM) and 40 molecules of CHOL (3:1:1:1:1). This specific molecular composition is a compromise in order for the membrane to be composed of the main phospholipid types a membrane might have (Meer et al. 2008). With respect to the glycerolipids, the palmitoyl chain located in the sn-1 position is completely saturated, whereas the oleoyl chain located in the sn-2 position contains a cis double bond between the C9 and C10 carbons. The presence of the oleoyl chain in the sn-2 position increases the overall mobility of the hydrocarbon chains of the phospholipids and hence fluidity in the xy plane of the membrane. The phospholipid/cholesterol ratio chosen represents 8.6 wt% of cholesterol in the sample. Cholesterol is an indispensable molecule for the

organization and organization of the membrane and modifies the physico-chemical properties of the lipid bilayer. However, there are many different phospholipid/cholesterol ratios found in biological membranes, from less than 5 wt% (ER, mitochondria) to more than 40 wt% (erythrocyte), so that we have taken a compromise. In this way, the cholesterol content we have used does not affect largely the simulation time scale but better simulates a model biomembrane. 37,914 molecules of water surrounded the membrane system. The solvent-to-lipid ratio in our system was 79, i.e. water as in excess (Murzyn et al. 2001). The bilayer and the bilayer normal lied in the xy plane and was parallel to the *z*-axis, respectively. Initially the simulation box had the dimensions of 12.1 and 12.4 nm in the *x*- and *y*-directions, respectively and 10.8 nm in the *z*-direction. The cross sectional area and the height of the simulation box were allowed to vary independently of each other. Each water layer, due to periodic boundary conditions, had an average dimension of 4 nm between membranes. CDDO-Me was created and minimized using Discovery Studio 4.0 software (Accelrys Inc., San Diego, USA). ParamChem (Vanommeslaeghe et al. 2010) was used to obtain the CHARMM General Force Field (CGenFF) compatible stream file of CDDO-Me which contained the optimized parameter and topology data of the molecule (using the PDB Reader plugin, Charmm-Gui web server, https://www.charmm-gui.org (Kim et al. 2017; Wu et al. 2014). The AutoPSF plugin for VMD (Humphrey et al. 1996) utilised the CDDO-Me stream file data to obtain the psf and pdb files of CDDO-Me required to build the whole system. Figure 1a shows the structure and carbon numbering of the CDDO-Me molecule. The lipid membrane model was prepared using the Charmm-Gui web server (https://www.charmm-gui.org, (Wu et al. 2014)). The system, at the beginning of the molecular simulation, contained 18 molecules of CDDO-Me (Fig. 1b). They were located at specific positions, i.e. 6 in the upper water layer, 6 in the lower water layer and 6 at the middle of the membrane bilayer. The {x, y, z} separation between different CDDO-Me molecules in the original system was {~ 28 Å, ~ 56 Å, ~ 34 Å}. The average distance between CDDO-Me molecules in water and the membrane surface was ~ 16 Å. Several CDDO-Me molecules were embedded at the middle of the membrane since it is known that CDDO-Me has a highly hydrophobic character (see above). This configuration is conveniently suited for the study of the interaction of small molecules with lipids in the membrane (Galiano and Villalain 2015, 2016; Kosinova et al. 2012). The system contained 80 sodium ions so that the system was electrostatically neutral.

Data Analysis

The layer of the phospholipid phosphate atoms defined the surface of the membrane and they were parallel to the {xy}

plane. The average distance between the phosphate atoms of the opposite leaflets defined the bilayer thickness, and the bilayer centre was defined by the centre-of-mass of the phosphate atoms of all the phospholipids ($z = 0$). The z-distance of the centre-of-mass of the CDDO-ME molecule relative to the bilayer centre was used to study its spatial position in the membrane. The membrane relative alignment of CDDO-Me was measured by the angle formed by the z-axis and the vector defined by carbons C3 and C21 of the CDDO-Me molecule (Fig. 1a). Visual Molecular Dynamics (VMD) (Humphrey et al. 1996) and Pymol were used for visualization and analysis. The radial distribution function, number of molecular contacts, S_{CD} order parameters, membrane thickness, diffusion coefficients, thickness two-dimensional maps, molecular areas, centre-of-mass, molecule tilt, surface area per lipid, and mass density profiles were obtained using the VMD Membplugin (Guixa-Gonzalez et al. 2014) as described in (Villalain 2019). Specifically, the S_{CD} order parameter tool calculates the carbon–deuterium order parameter, $S_{CD} = -\frac{1}{2}\langle 3cos^2\theta - 1\rangle$, a value that reflects the orientational mobility of each C-H bond along the aliphatic phospholipid tail and thus membrane fluidity (Guixa-Gonzalez et al. 2014). The condition employed to determine the presence of hydrogen bonds was a distance less than 2.5 Å between donor and acceptor atoms and a donor-H-acceptor angle of at least 150° (Baylon and Tajkhorshid 2015). The analyses were performed over the whole MD simulation unless otherwise indicated.

Results

Membrane Equilibration

To evaluate the suitability of the simulation methodology and check the equilibration of the membrane system we studied the time variation of the area per lipid (Anézo et al. 2003; Kandt et al. 2007). The time plots of the molecular area corresponding to the upper (z+) and lower (z−) leaflets of the bilayer for all the lipids, i.e. POPC, POPE, POPS, PSM and CHOL, are shown in Fig. 2a and b, respectively. No substantial changes were found in the bilayer properties of this very diluted system: the model membrane has 560 lipid molecules and 18 CDDO-Me molecules, 12 of them outside the membrane, so that the lipid/CDDO-Me relationship in the membrane is approximately 93:1. The data show that both cholesterol and phospholipids were equilibrated early on the course of the simulation, both at the z+ and at the z− bilayer leaflets, indicating that the membrane system reached a steady state after ~25–30 ns of simulation. At the end of the simulation, the mean area of POPC, POPE, POPS, PSM and CHOL for the upper and lower leaflets were 57.8 ± 1.3 and 57.5 ± 1.1 Å^2, 57.4 ± 1.7 and 56.9 ± 2.1 Å^2,
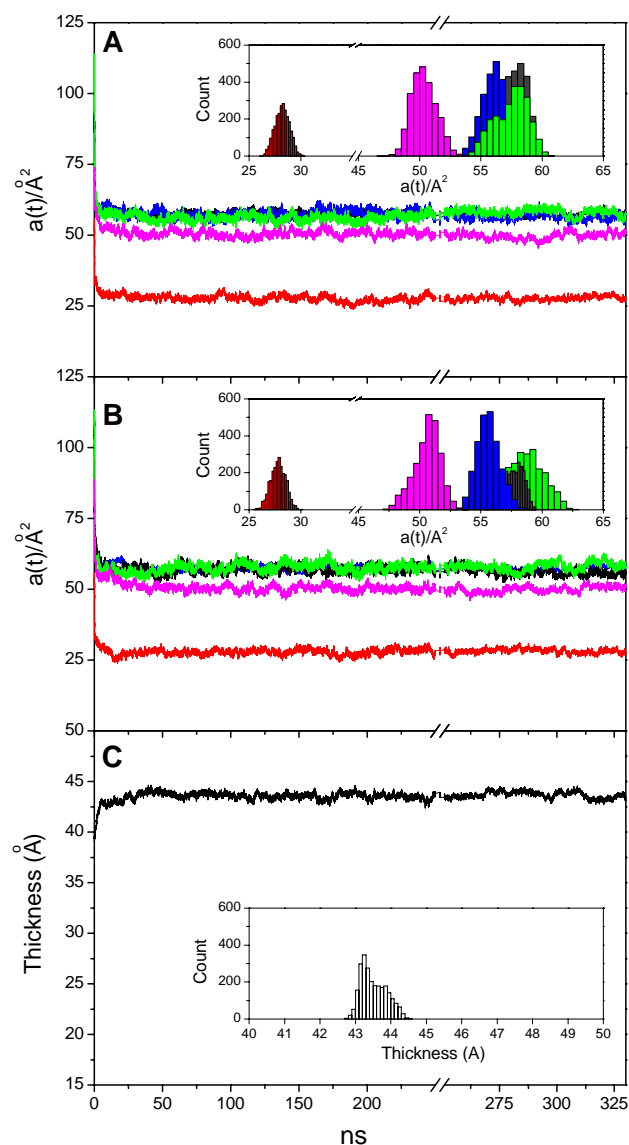
Fig. 2 Time variation of the (**a**, **b**) molecular areas for each lipid species in the POPC/POPE/POPS/PSM/CHOL system for the (**a**) z+ and (**b**) z− leaflets of the bilayer and (**c**) the total membrane thickness. The inserts in **a**, **b** and **c** show the last 25 ns histograms of the molecular areas variation for the (**a**) z+ and **b** z− leaflets of the bilayer and the **c** total membrane thickness, respectively. In (**a**) and (**b**) POPC, POPE, POPS, PSM and CHOL data are drawn in black, blue, green, magenta and red, respectively

56.7 ± 2.0 and 57.7 ± 1.9 Å^2, 50.4 ± 1.5 and 55.5 ± 1.8 Å^2 and 27.8 ± 1.3 and 27.9 ± 1.2 Å^2, respectively (Fig. 2a and b, inserts). These values were comparable to those reported previously (Bera and Klauda 2017; Mukhopadhyay et al. 2004). Similarly, membrane thickness remained reasonably constant after ~30–35 ns (Fig. 2c). The average membrane thickness for the last 25 ns was 43.5 ± 0.4 Å (Fig. 2c, insert), similar to those reported for CHOL containing systems (Bera and Klauda 2017).

CDDO-Me Behaviour

At the beginning of the simulation, the CDDO-Me molecules were positioned in the superior water layer (6 molecules), in the inferior water layer (6 molecules) and in the central part of the membrane (6 molecules) (see Fig. 1b). The final ($t = 325$ ns) snapshot for the POPC/POPE/POPS/PSM/CHOL membrane model system containing the CDDO-Me molecules is shown in Fig. 1c. At the end of the simulation, the CDDO-Me molecules relocated to a position near the membrane interface. In this case, the cyano groups of the CDDO-Me molecules were located near the ester groups of the molecules of phospholipid, and extended to the interior part of the membrane without reaching the middle of the phospholipid hydrocarbon acyl chains (Fig. 1c). Quite the opposite, all molecules of CDDO-Me, which were located in the upper and lower water layers at the beginning of the simulation, aggregated with time; all of them combined in an ensemble of twelve CDDO-Me molecules at the end of the simulation (Fig. 1c). It is clear from these pictures that CDDO-Me aggregates in water, it does not aggregate when it is inside the membrane and, significantly, locates in a relative oblique position at the upper part of the membrane.

The dissimilar behaviour observed for the CDDO-Me molecules in and out of the membrane is observed in the time change of the centre-of-mass of the CDDO-Me molecules if we compare them with the z+ and z− phosphate atoms centre-of-mass (Fig. 3a). The CDDO-Me molecules which were initially located at the middle of the upper and water layers, i.e. molecules 1 to 6 and molecules 13 to 18, displayed a substantial fluctuation in their centre-of-mass, variation which was maintained throughout the whole simulation (Fig. 3a). As an example, the histogram corresponding to the centre-of-mass of CDDO-Me molecule no. 17 for the
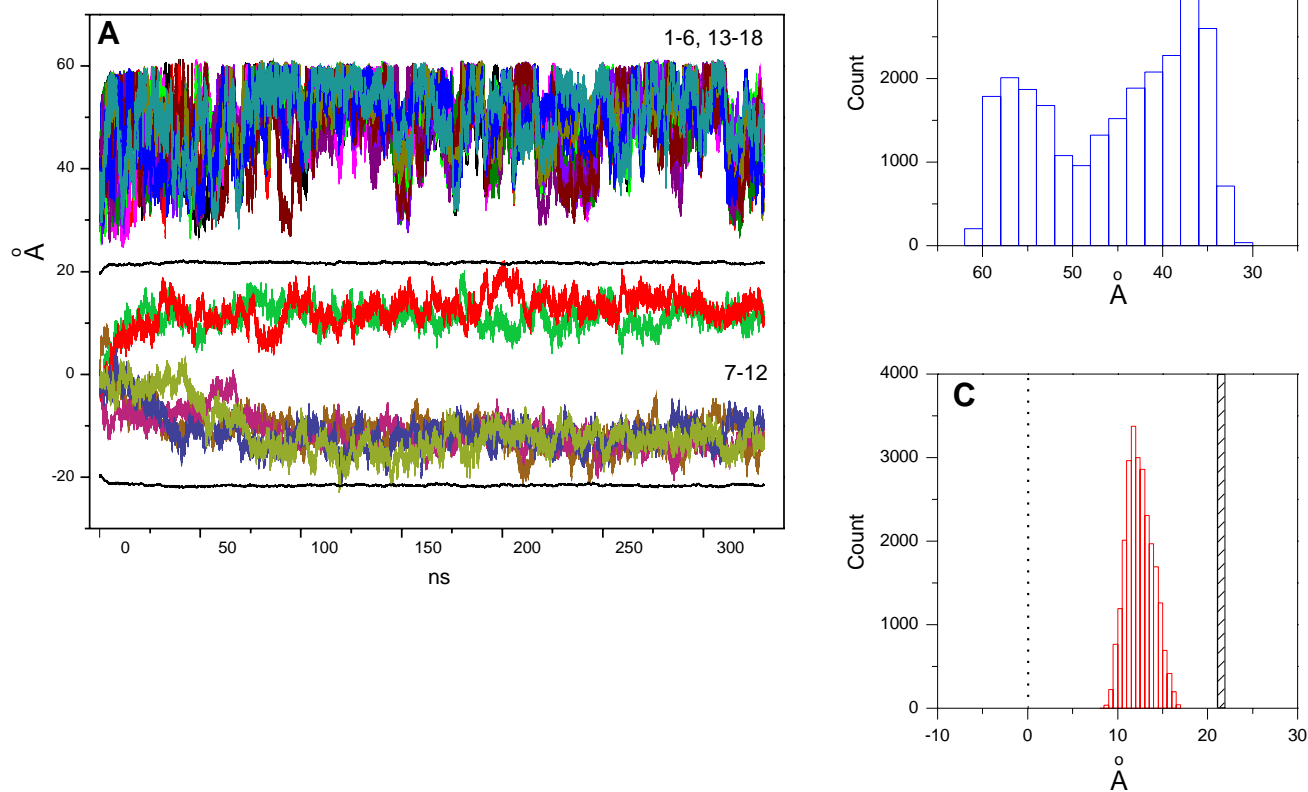
Fig. 3 **a** Change of the centre-of-mass of the eighteen CDDO-Me molecules in the POPC/POPE/POPS/PSM/CHOL membrane model system for the whole simulation (each color refers to a molecule of CDDO-Me in the system). To compare the CDDO-Me molecules 1 to 6 and 13 to 18 centre-of-masses, the absolute values are represented. The black lines represent the centre-of-mass of the phosphate atoms at the z+ and the z− leaflets. **b** and **c** show the last 25 ns histograms of the centre-of-masses of CDDO-Me molecules no. 17 (blue in (**a**)) and no. 10 (red in (**a**)), respectively. The upper membrane boundary defined by the phosphate atoms (patterned box) and the centre of the bilayer (dotted line) are shown in the histogram of the CDDO-Me molecule no. 10. Note the identical value span for distances in the abscissa axis

last 25 ns of the simulation is shown in Fig. 3b. The pattern of the centre-of-mass values of the other CDDO-Me molecules in the water layers were similar to that of molecule no. 17 (Fig. 3a). The distribution is a significant one because these CDDO-Me molecules are completely free to move. In addition and upon time, they completely aggregate. At the beginning they formed dimers and trimers and later on all of them formed a massive aggregate of twelve CDDO-Me molecules. In contrast, those molecules which were initially located at the middle of the bilayer, molecules 7 to 12, moved to a similar average location in a short space of time (Fig. 3a). This location, similar for all of them, was between the middle of the hydrocarbon chains and the ester groups of the phospholipids. It is important to emphasize that at no time none of these CDDO-Me molecules aggregated, in contrast to the molecules in solution. Moreover, the dispersion of their location was significantly lower than that of the CDDO-Me molecules in water as proved by the histogram of the centre-of-mass of CDDO-Me molecule no. 10 for the last 25 ns (compare Fig. 3b and c). These CDDO-Me molecules equilibrated between 40 and 75 ns in a position that remained relatively constant and in a relatively similar position along the whole simulation, i.e. between 7 and 19 Å from the centre of the bilayer (Fig. 3a). The dispersion in the location of the CDDO-Me molecules in the membrane was significantly lower than that of the CDDO-Me molecules in water. Whereas it was about 7–9 Å for the former, it was about 30–35 Å for the latter. These data would also indicate that the CDDO-Me molecules inside the membrane were in a stable location after 75 ns. Taking into account that (a) the CDDO-Me molecule is a relatively rigid one, (b) the CDDO-Me molecule does not completely span the leaflet of the bilayer and (c) the length between its carbons C3 and C21 (cf. Fig. 1a) is about 11.5 A, its disposition inside the membrane tends to be placed in an intermediate position between parallel and perpendicular to the membrane, i.e. in an oblique position (see below).

The representation of the number of CDDO-Me molecules which were next to each other for each one the CDDO-Me molecules for all the simulation time is shown in Supplementary Fig. 1A. It is possible to observe that, for each one of the CDDO-Me molecules, the number of next molecules increase upon time, indicating that they were aggregating until a maximum number was encountered. The time to attain the maximum number of next molecules varied between different CDDO-Me molecules, from a minimum of about 100 ns to a maximum of about 250 ns (Supplementary Fig. 1A). This time would obviously depend on the difference in distance between the different CDDO-Me molecules at the beginning of the simulation time. It is interesting to observe the great variation in next molecules for each one of the CDDO-Me molecules. This variation implies that different CDDO-Me approximates to each other but also they move away along the simulation time. For example, CDDO-Me molecule no. 14 approximates to 8 other CDDO-Me molecules up to 140 ns; from 140 to 170 ns it moves away so that there are no CDDO-Me molecules next to it, and after 170 ns, it approximates to other CDDO-Me molecules until all them collapse in one big aggregate. Therefore, at the end of the simulation time, CDDO-Me molecule no. 14, together with the other 11 CDDO-Me molecules, is forming a composite of 12 CDDO-Me molecules (Supplementary Fig. 1A-14). The maximum number of next molecules for each one of the CDDO-Me molecules for the last 25 ns of the simulation is shown in Supplementary Fig. 1B. From these data, it can be inferred that, on average, for each CDO-Me molecule the number of next CDDO-Me molecules was ~ 9. These data highlight the significant propensity of the CDDO-Me molecules to aggregate in solution but not in the membrane. It is interesting to note here that several works have used CDDO-Me in drinking water for animal experimentation (see for example (Camer et al. 2016)). The formation of a complex aggregate in solution might hamper the antiviral, antimicrobial and anticancer effects of CDDO-Me and therefore a convenient vehicle for its formulation should be used in clinical assays.

We have studied the number of contacts between CDDO-Me molecules along the whole simulation and the results are shown in Supplementary Fig. 2. As it is observed in the figure, molecules of CDDO-Me no. 1 to 6 and no. 13 to 18 present a significant number of contacts between them but molecules of CDDO-Me no. 7 to 12, i.e. CDDO-Me molecules inside the membrane, do not present any type of contact between them at any time during the simulation. Supplementary Fig. 3 presents the total number of contacts between all CDDO-Me molecules during the last 25 ns of the simulation. Again, CDDO-Me molecule no. 7 to 12 do not present any type of contact with any other CDDO-Me molecule in the system, whereas the CDDO-Me molecules in the water layer present a significant number of contacts between them (average number of 3664 ± 997). These data highlight again the propensity of CDDO-Me to aggregate in solution but certainly not in the membrane.

We have obtained the diffusion coefficients of the membrane phospholipids and the CDDO-Me molecules by using their averaged mean square displacement for the last 25 ns. The diffusion coefficient for POPC was 6.2 μm^2/s, 5.9 μm^2/s for POPE, 5.6 μm^2/s for POPS, 5.5 μm^2/s for PSM and 5.9 μm^2/s for CHOL, values similar to those previously reported (Gielen et al. 2009; Wang et al. 2011). In the case of CDDO-ME inside the membrane the diffusion coefficient was 10.7 μm^2/s whereas for those CDDO-Me molecules outside it, i.e. in the water layer, it was 141.8 μm^2/s. In the case of CDDO-Me inside the membrane its average diffusion was about 1.8 times the diffusion coefficient of the lipids, whereas for CDDO-Me in the water layer it was about 24 times more.

This difference in diffusion coefficient values would explain the ease of CDDO-Me molecules to interact with each other and form an aggregate in solution.

Membrane Mass Density Profiles

The average last 25 ns of the mass density profiles for all the components in the biomembrane model system is shown in Fig. 4a. As observed in the figure, the molecules of CDDO-Me form three different populations, two of them inside the membrane and the other one outside (membrane boundaries defined by the mass density profile of the phospholipid atoms). The outer population of CDDO-Me molecules correspond to those molecules which aggregate as the simulation time elapses. The average location of the CDDO-Me molecules inside the membrane lies from about 19 Å to 7 Å of the centre of the bilayer (Fig. 4a). They lie on average at a location which is lower than the phosphate groups of the phospholipids but they never reach the centre of the bilayer, their location being relatively similar to the location

of the CHOL molecules (Fig. 4a). The bandwidth of the mass density profiles of these CDDO-Me molecules were different, which would imply a similar location but slightly different orientation (see below). The mass density profiles corresponding to the phosphate atoms for each type of phospholipid in the system is shown in Fig. 4b. There are subtle differences between the average locations of the phosphate atoms, remarkable in the second derivative of the mass density profiles (insert, Fig. 4b). All of the profiles are rather symmetric except for the z− layer phosphates pertaining to the POPE phospholipids, which would imply the existence of at least two different populations of POPE. The maxima of the mass density profile for the average location of POPC phosphates are at 22.47 Å and − 21.51 Å, for POPE phosphates are at − 21.51 Å and 21.4 Å, for POPS phosphates are at − 21.05 Å and 21.04 Å, and finally for PSM phosphates are at − 22.7 Å and 22.04 Å. The differences in the maxima of the mass density profiles are greater at the z+ layer than at the z− one. In a significant way, these data would imply the existence of differences in the location of the phosphate
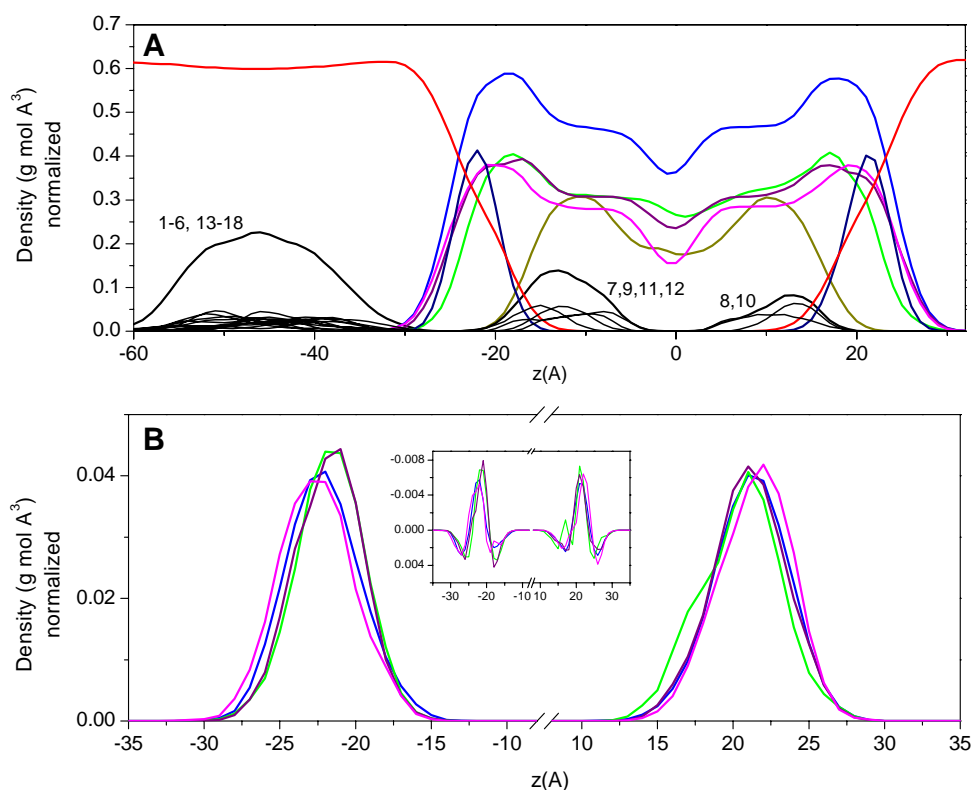
Fig. 4 Mass density profiles for the last 25 ns of the simulation for the system containing POPC/POPE/POPS/PSM/CHOL and the eighteen CDDO-Me molecules. **a** Mass density profiles corresponding to water (red), POPC (blue, multiplied by 2), POPE *(*green, multiplied by 4), POPS (purple, multiplied by 4), PSM (magenta, multiplied by 4), CHOL (dark yellow, multiplied by 4), phospholipid phosphate atoms (navy, multiplied by 5) and all CDDO-Me molecules (black, multiplied by 10). The CDDO-Me molecules are numbered and each

individual density profile is shown, as well as its sum. **b** Expansion of the mass density profiles corresponding to the phosphate groups of POPC (blue), the phosphate groups of POPE (green, multiplied by 3), the phosphate groups of POPS (purple, multiplied by 3) and the phosphate groups of PSM (magenta, multiplied by 3). The insert shows the second derivative of the mass density profiles of the corresponding phosphate groups

atoms depending both on phospholipid type and layer. This could be associated to the fact that the number of CDDO-Me molecules at the end of the simulation is greater at the z+ layer (CDDO-Me molecules no. 7, 9, 11 and 12) than at the z− one (CDDO-Me molecules no. 8 and 10).

CDDO-Me Orientation in the Membrane

The alignment of the CDDO-Me molecules in the membrane was studied considering the angle formed by the membrane z-axis and the molecular axis defined by the vector joining carbons 3 and 21 of CDDO-Me (see Fig. 1). As expected, those molecules in solution showed a great deviation in angle, ranging from a minimum value of about 0° and a maximum of about 180°, i.e. nearly all possible orientations (not shown for briefness). At no moment there was any convergence pattern, implying that their movement was completely free, except when they were aggregated since

they behaved as an unit. Even when all twelve CDDO-Me molecules were aggregated the dispersion of their tilt angles was a significant one implying no orientation preference. In contrast, a completely different behaviour was observed for the CDDO-Me molecules inside the membrane. Figure 5 shows the tilt angle of those molecules for the last 25 ns of the molecular dynamics simulation. As observed in the figure, their tilt angle displayed two relatively definite angles, $53.4 \pm 19.7°$ and $119.1 \pm 21.8°$, i.e. all CDDO-Me molecules inside the membrane presented an oblique position. These data stress again the complete different behaviour of CDDO-Me in solution and inside the membrane.

CDDO-ME/Lipid Interaction

The average number of POPC molecules within 7 Å of the membrane CDDO-Me molecules was 1.22, whereas it was 0.55 for POPE, 0.75 for POPS, 0.33 for PSM and
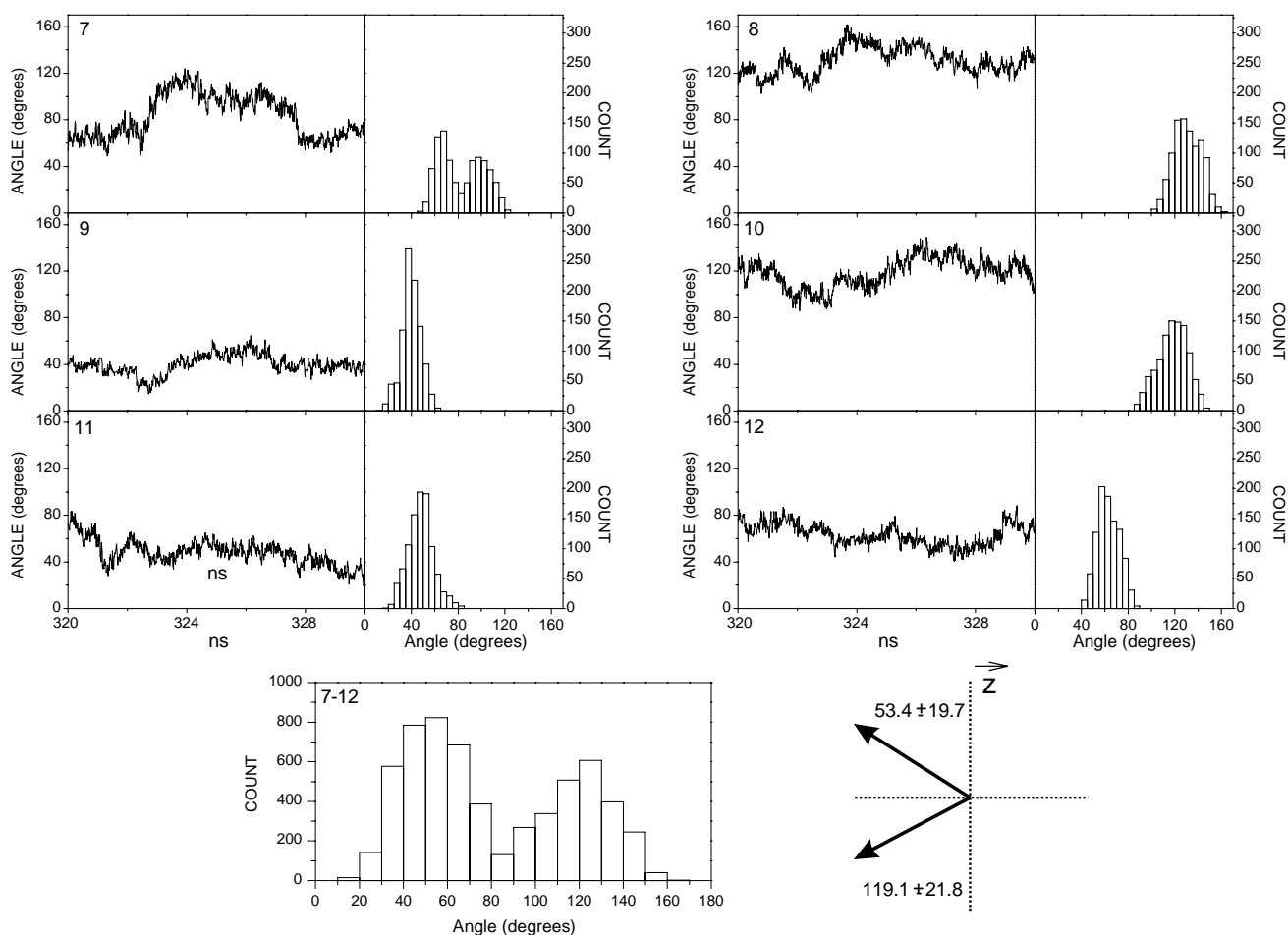
Fig. 5 Time variation of the tilt angle with respect to the perpendicular of the membrane surface and their corresponding histograms for the last 25 ns of the simulation for CDDO-Me molecules no. 7-12 as indicated. The lower part of the figure presents the combination of all data as well as the obtained average tilt angle. The tilt angle is defined by the vector joining the membrane z-axis and carbons C3 and C21 of CDDO-Me. See text for details

0.38 for CHOL. These data give a relationship of about 3.7:1.7:2.3:1:1.1, which can be compared with the total number of different lipids in the system, i.e. 3:1:1:1:1. Any deviation from the 3:1:1:1:1 relationship would indicate the preference for some lipids to remain close to the CDDO-Me molecules upon time, implying the existence of a specific interaction between CDDO-Me and the lipids. Since the average number of POPC molecules was 1.22, to maintain the original 3:1:1:1:1 relationship the average number of the other molecules should be around 0.406. The average number of PSM and CHOL molecules is 0.33 and 0.38, respectively, so it could be confidently assumed that there is no specific interaction of CDDO-Me with these phospholipid molecules. However, the average number of POPE and POPS molecules is 0.55 and 0.75, respectively, which is much higher than 0.406. These data would imply the presence of a specific interaction between CDDO-Me and both POPE and POPS phospholipids.

We have obtained the radial distribution function, $g(r)$, for each lipid molecule in the system in order to know the likelihood to find each lipid type respect to CDDO-ME (Supplementary Fig. 4). For the first 25 ns of simulation, the most intense signal originates from POPE, followed by POPS and POPC (Supplementary Fig. 4 A). For POPE the highest $g(r)$ value of 3.25 appears at about 6.91 Å. At this distance, POPS and POPC present $g(r)$ values of 2.62 and 2.25, whereas PSM and CHOL present $g(r)$ lower values of 1.32 and 1.10. For the last 25 ns of simulation (Supplementary Fig. 4B), the most intense signal originates from POPS, the highest $g(r)$ value of 3.76 appearing at about 8.7 Å; the $g(r)$ values of all the other lipids present lower values at all distances. At 8.7 Å POPE shows a $g(r)$ value of 2.79 whereas POPC, PSM and CHOL present $g(r)$ values of 2.11, 1.36 and 1.11, respectively. These data indicate that, at the beginning of the simulation, POPE and to a lesser extent POPS and POPC had the highest probability to be found near the CDDO-Me molecules. However, at the end of the simulation, POPS and to a lesser extent POPE were the lipids which had the greater probability to be found around the CDDO-Me molecules in the membrane. POPC, PSM and CHOL, in this order, have lower probabilities to be associated with CDDO-Me.

We have also calculated the average normalized number of hydrogen bonds per CDDO-Me molecule and the membrane lipids (not shown for briefness). For the last 25 ns of simulation time the number of hydrogen bonds between CDDO-Me and POPC is 1.83 ± 0.66, whereas the number of hydrogen bonds between CDDO-Me and POPE is 4.83 ± 0.26. For the other lipids, no hydrogen bonds were found between them and CDDO-Me. These data would demonstrate the existence of a specific interaction between CDDO-Me and POPE in the membrane and corroborate the data mentioned above, i.e. CDDO-Me interact specifically with POPE and POPS in the membrane.

Effect of CDDO-Me on Lipid Hydrocarbon Chain Order

Since any molecule inserted in the membrane can affect the hydrocarbon chain order of the phospholipid acyl chains, we have obtained their $-S_{CD}$ order parameters in the presence of CDDO-Me (Fig. 6). An $-S_{CD}$ value of 0 indicates an isotropic orientation, a value of 0.5 indicates full order along the normal bilayer and a value of -0.25 indicates full order along the bilayer plane (Tieleman et al. 1997). The average $-S_{CD}$ values of the acyl chains of all phospholipids far from the CDDO-Me molecule, i.e. in the bulk membrane model system, are according to the profiles observed earlier for both simulated and experimental data (Bockmann et al. 2003; Klauda et al. 2010; Tsai et al. 2015). There were no dramatic effects on the order parameter of the POPC hydrocarbon chains next to the CDDO-Me molecules; however, they slightly reduce the $-S_{CD}$ values along the whole hydrocarbon chains (Fig. 6a and b). The effect observed on the POPE (Fig. 6c and d) and POPS (Fig. 6e and f) molecules next to the CDDO-Me molecules was similar to those observed for POPC, since their presence slightly reduced the $-S_{CD}$ values along the hydrocarbon chains. A similar effect was observed for (Fig. 6g). From these data it can be inferred that the CDDO-Me molecules are inserted relatively well between the phospholipid hydrocarbon chains but reduce to some extent their anisotropy, i.e. increase their fluidity. The differences in order parameter which we have found might reflect the long-range effects produced by the CDDO-Me molecules in the membrane.

Discussion

Many molecules, such as CDDO-Me, displaying hydrophobic and/or amphipathic structures have a tendency to bind and insert into biomembranes. Therefore these molecules have a significant effect on the membrane biophysical properties. These amphipathic/hydrophobic molecules do interact, apart with different types of proteins, with the membrane and its components, the phospholipids (Kopec et al. 2013; Tsuchiya 2015). The number of different biological effects these molecules have imply that they affect different mechanisms but also point out to the existence of a common target which should be the biological membrane. Their interactions with membrane lipids and the modulation of the membrane physico-chemical properties should play a fundamental role in the biological activities these bioactive molecules display. Their biological, pharmacological and medicinal properties would be related

Fig. 6 Average deuterium order parameter $-S_{CD}$ calculated for the *sn*-1 (**a**, **c**, **e**) and *sn*-2 (**b**, **d**, **f** acyl chains of (**a**, **b**) POPC, **c**, **d** POPE and **e**, **f** POPS within 7 Å of the CDDO-Me molecules (unfilled square) compared to the bulk phospholipid acyl chains (filled square). **g** Average deuterium order parameter $-S_{CD}$ calculated for the sphyngosyl acyl chain of PSM within 7 Å of the CDDO-Me molecules (unfilled square) compared to the bulk PSM sphyngosyl acyl chain (filled square). The analysis was carried out for the last 25 ns of simulation
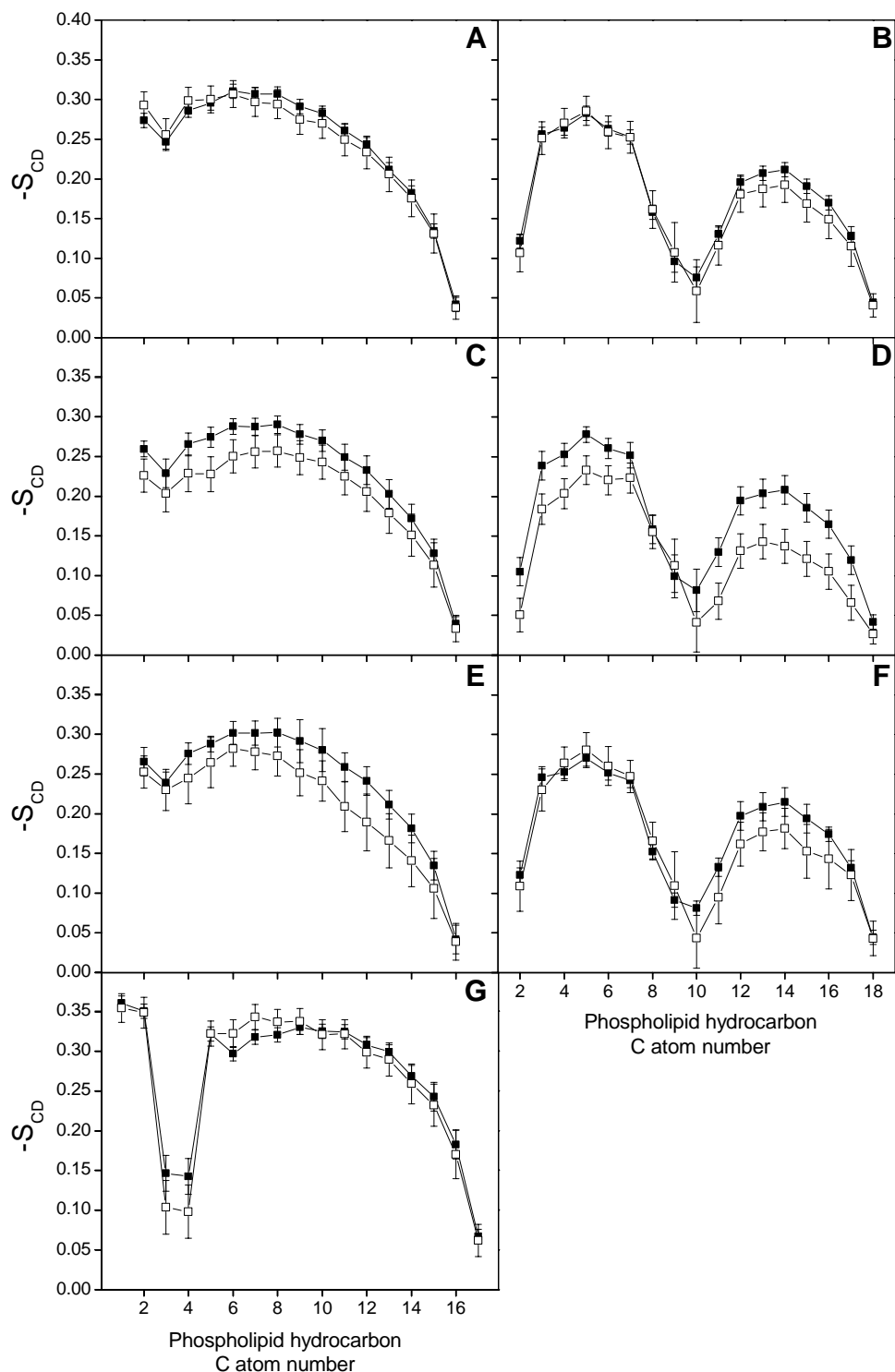
to this membrane modulation effect which itself would depend on their location, their orientation, their interactions and their structure in the membrane (Margina et al. 2012; Tsuchiya 2015). Interestingly, CDDO-Me has displayed a promising activity for the treatment of cancer (Deeb et al. 2009; Gao et al. 2015; Hong et al. 2012;

Mathis and Cui 2016; Wang et al. 2014). It is also worth noting that CDDO-Me can induce apoptosis in leukaemia cells at the same time that an increase in annexin V staining is observed, pointing out to an increase of phosphatidylserine at the membrane surface (Jin et al. 2017). This would be related to the fact that phosphatidylserine and

phosphatidylethanolamine phospholipids reside primarily in the inner leaflet of normal eukaryotic cells, but their distribution changes dramatically in cancer cells, moving towards the outer membrane leaflet (Schutters and Reutelingsperger 2010; Utsugi et al. 1991). It is also worth noting that CDDO-Me can induce apoptosis in leukaemia cells at the same time that an increase in annexin V staining is observed, pointing out to an increase of phosphatidylserine at the membrane surface (Jin et al. 2017). The specific interaction of CDDO-Me with phosphatidylserine and phosphatidylethanolamine in the membrane might cause problems of mobility and activity to different types of proteins (Leth-Larsen et al. 2010; Zalba and Hagen 2017) leading to the specific effect CDDO-Me has on cancer cells. Therefore, the biological properties of CDDO-Me should therefore be attributed to its capability to modify the membrane biophysical properties through interaction with specific phospholipids.

In this work we intended to locate the molecule of CDDO-Me in the membrane and determine the specific interactions of the molecule with membrane lipids using molecular dynamics simulations. For that goal, we have used a model membrane composed of the phospholipids POPC, POPE, POPS, PSM, as well as CHOL, providing us with a detailed evidence on the nature of the interactions and location of CDDO-Me in the membrane. Although our membrane model system does not account for the presence of proteins or the fact that biological membranes have an asymmetrical distribution of lipids in the two monolayers, our results support that CDDO-Me tends to locate in the middle of the hydrocarbon layer of the membrane without reaching the middle of the membrane. CDDO-Me molecules have a tendency to be oriented in such a way that they are in an oblique position; their cyano groups lean towards the membrane surface and the methyl esther groups towards the middle of the membrane. In the membrane the CDDO-Me molecules mostly interact preferentially with phosphatidylserine and phosphatidylethanolamine phospholipids and this interaction might lead to the specific effect CDDO-Me has on cancer cells. Furthermore, in our membrane system, the approximate concentration of CDDO-Me in water is 17 mM and in the membrane 20 mM. This concentration is certainly higher than what could be found in the clinic (Hong et al. 2012) but considering the difference in diffusion coefficient of CDDO-Me in solution and in the membrane (about 13 times higher in solution than in the membrane) it gives us a clue to its different behaviour in both media. The formation of a complex aggregate in solution for the CDDO-Me molecules might impede its antiviral, antimicrobial and anticancer activities and therefore it should be taken into account when intended to be used in clinical assays so to choose a convenient vehicle for its formulation. Our work should aid in the development of these molecules opening new avenues for future therapeutic advances.

Compliance with Ethical Standards

References

Anézo C, de Vries AH, Höltje H-D, Tieleman DP, Marrink S-J (2003) Methodological issues in lipid bilayers simulations. J. Phys. Chem. B 107:9424–9433

Baylon JL, Tajkhorshid E (2015) Capturing spontaneous membrane insertion of the influenza virus hemagglutinin fusion Peptide. J Phys Chem B 119:7882–7893

Bera I, Klauda JB (2017) Molecular simulations of mixed lipid bilayers with sphingomyelin, glycerophospholipids, and cholesterol. J Phys Chem B 121:5197–5208

Best RB, Zhu X, Shim J, Lopes PE, Mittal J, Feig M, Mackerell AD Jr (2012) Optimization of the additive CHARMM all-atom protein force field targeting improved sampling of the backbone phi, psi and side-chain chi(1) and chi(2) dihedral angles. J Chem Theory Comput 8:3257–3273

Bockmann RA, Hac A, Heimburg T, Grubmuller H (2003) Effect of sodium chloride on a lipid bilayer. Biophys J 85:1647–1655

Camer D, Yu Y, Szabo A, Wang H, Dinh CH, Huang XF (2016) Bardoxolone methyl prevents obesity and hypothalamic dysfunction. Chem Biol Interact 256:178–187

Chin MP, Reisman SA, Bakris GL, O'Grady M, Linde PG, McCullough PA, Packham D, Vaziri ND, Ward KW, Warnock DG, Meyer CJ (2014) Mechanisms contributing to adverse cardiovascular events in patients with type 2 diabetes mellitus and stage 4 chronic kidney disease treated with bardoxolone methyl. Am J Nephrol 39:499–508

de Zeeuw D, Akizawa T, Audhya P, Bakris GL, Chin M, Christ-Schmidt H, Goldsberry A, Houser M, Krauth M, Lambers Heerspink HJ, McMurray JJ, Meyer CJ, Parving HH, Remuzzi G, Toto RD, Vaziri ND, Wanner C, Wittes J, Wrolstad D, Chertow GM, Investigators BT (2013) Bardoxolone methyl in type 2 diabetes and stage 4 chronic kidney disease. N Engl J Med 369:2492–2503

Deeb D, Gao X, Jiang H, Dulchavsky SA, Gautam SC (2009) Oleanane triterpenoid CDDO-Me inhibits growth and induces apoptosis in prostate cancer cells by independently targeting pro-survival Akt and mTOR. Prostate 69:851–860

Dzubak P, Hajduch M, Vydra D, Hustova A, Kvasnica M, Biedermann D, Markova L, Urban M, Sarek J (2006) Pharmacological activities of natural triterpenoids and their therapeutic implications. Nat Prod Rep 23:394–411

Galiano V, Villalain J (2015) Oleuropein aglycone in lipid bilayer membranes. A molecular dynamics study. Biochim Biophys Acta 1848:2849–2858

Galiano V, Villalain J (2016) The location of the protonated and unprotonated forms of arbidol in the membrane: a molecular dynamics study. J Membr Biol 249(3):381–391

Gao X, Deeb D, Liu Y, Liu P, Zhang Y, Shaw J, Gautam SC (2015) CDDO-Me inhibits tumor growth and prevents recurrence of pancreatic ductal adenocarcinoma. Int J Oncol 47:2100–2106

Gielen E, Smisdom N, van de Ven M, De Clercq B, Gratton E, Digman M, Rigo JM, Hofkens J, Engelborghs Y, Ameloot M (2009) Measuring diffusion of lipid-like probes in artificial and natural membranes by raster image correlation spectroscopy (RICS): use of a commercial laser-scanning microscope with analog detection. Langmuir 25:5209–5218

Guixa-Gonzalez R, Rodriguez-Espigares I, Ramirez-Anguita JM, Carrio-Gaspar P, Martinez-Seara H, Giorgino T, Selent J (2014) MEMBPLUGIN: studying membrane complexity in VMD. Bioinformatics 30:1478–1480

Hong DS, Kurzrock R, Supko JG, He X, Naing A, Wheler J, Lawrence D, Eder JP, Meyer CJ, Ferguson DA, Mier J, Konopleva M, Konoplev S, Andreeff M, Kufe D, Lazarus H, Shapiro GI, Dezube BJ (2012) A phase I first-in-human trial of bardoxolone methyl in patients with advanced solid tumors and lymphomas. Clin Cancer Res 18:3396–3406

Huang Z, Mou Y, Xu X, Zhao D, Lai Y, Xu Y, Chen C, Li P, Peng S, Tian J, Zhang Y (2017) Novel derivative of bardoxolone methyl improves safety for the treatment of diabetic nephropathy. J Med Chem 60:8847–8857

Humphrey W, Dalke A, Schulten K (1996) VMD: visual molecular dynamics. J Mol Graph 14(33–8):27–28

Itokawa H, Morris-Natschke SL, Akiyama T, Lee KH (2008) Plant-derived natural product research aimed at new drug discovery. J Nat Med 62:263–280

Jin UH, Cheng Y, Zhou B, Safe S (2017) Bardoxolone methyl and a related triterpenoid downregulate cMyc expression in leukemia cells. Mol Pharmacol 91:438–450

Jorgensen WLC, Madura J, Klein ML (1983) Comparison of simple potential functions for simulating liquid water. J. Chem. Phys. 79:926–935

Kandt C, Ash WL, Tieleman DP (2007) Setting up and running molecular dynamics simulations of membrane proteins. Methods 41:475–488

Kim S, Lee J, Jo S, Brooks CL 3rd, Lee HS, Im W (2017) CHARMM-GUI ligand reader and modeler for CHARMM force field generation of small molecules. J Comput Chem 38:1879–1886

Klauda JB, Venable RM, Freites JA, O'Connor JW, Tobias DJ, Mondragon-Ramirez C, Vorobyov I, MacKerell AD Jr, Pastor RW (2010) Update of the CHARMM all-atom additive force field for lipids: validation on six lipid types. J Phys Chem B 114:7830–7843

Kopec W, Telenius J, Khandelia H (2013) Molecular dynamics simulations of the interactions of medicinal plant extracts and drugs with lipid bilayer membranes. FEBS J 280:2785–2805

Kosinova P, Berka K, Wykes M, Otyepka M, Trouillas P (2012) Positioning of antioxidant quercetin and its metabolites in lipid bilayer membranes: implication for their lipid-peroxidation inhibition. J Phys Chem B 116:1309–1318

Leth-Larsen R, Lund RR, Ditzel HJ (2010) Plasma membrane proteomics and its application in clinical cancer biomarker discovery. Mol Cell Proteom 9:1369–1382

Liby KT, Sporn MB (2012) Synthetic oleanane triterpenoids: multifunctional drugs with a broad range of applications for prevention and treatment of chronic disease. Pharmacol Rev 64:972–1003

Margina D, Ilie M, Manda G, Neagoe I, Mocanu M, Ionescu D, Gradinaru D, Ganea C (2012) Quercetin and epigallocatechin gallate effects on the cell membranes biophysical properties correlate with their antioxidant potential. Gen Physiol Biophys 31:47–55

Mathis BJ, Cui T (2016) CDDO and its role in chronic diseases. Adv Exp Med Biol 929:291–314

Mukhopadhyay P, Monticelli L, Tieleman DP (2004) Molecular dynamics simulation of a palmitoyl-oleoyl phosphatidylserine bilayer with Na+ counterions and NaCl. Biophys J 86:1601–1609

Murzyn K, Rog T, Jezierski G, Takaoka Y, Pasenkiewicz-Gierula M (2001) Effects of phospholipid unsaturation on the membrane/water interface: a molecular simulation study. Biophys J 81:170–183

Peron G, Marzaro G, Dall Acqua S (2018) Known triterpenes and their derivatives as scaffolds for the development of new therapeutic agents for cancer. Curr Med Chem 25:1259–1269

Refaat A, Pararasa C, Arif M, Brown JE, Carmichael A, Ali SS, Sakurai H, Griffiths HR (2017) Bardoxolone-methyl inhibits migration and metabolism in MCF7 cells. Free Radic Res 51:211–221

Samudio I, Konopleva M, Pelicano H, Huang P, Frolova O, Bornmann W, Ying Y, Evans R, Contractor R, Andreeff M (2006) A novel mechanism of action of methyl-2-cyano-3,12 dioxoolean-1,9 diene-28-oate: direct permeabilization of the inner mitochondrial membrane to inhibit electron transport and induce apoptosis. Mol Pharmacol 69:1182–1193

Samudio I, Kurinna S, Ruvolo P, Korchin B, Kantarjian H, Beran M, Dunner K Jr, Kondo S, Andreeff M, Konopleva M (2008) Inhibition of mitochondrial metabolism by methyl-2-cyano-3,12-dioxooleana-1,9-diene-28-oate induces apoptotic or autophagic cell death in chronic myeloid leukemia cells. Mol Cancer Ther 7:1130–1139

Schutters K, Reutelingsperger C (2010) Phosphatidylserine targeting for diagnosis and treatment of human diseases. Apoptosis 15:1072–1082

Shanmugam MK, Dai X, Kumar AP, Tan BK, Sethi G, Bishayee A (2014) Oleanolic acid and its synthetic derivatives for the prevention and therapy of cancer: preclinical and clinical evidence. Cancer Lett 346:206–216

Sheng H, Sun H (2011) Synthesis, biology and clinical significance of pentacyclic triterpenes: a multi-target approach to prevention and treatment of metabolic and vascular diseases. Nat Prod Rep 28:543–593

The Pymol Molecular Graphics System, version 1.7.4. Schrödinger, LLC

Tieleman DP, Marrink SJ, Berendsen HJ (1997) A computer perspective of membranes: molecular dynamics studies of lipid bilayer systems. Biochim Biophys Acta 1331:235–270

Tsai HH, Lee JB, Li HS, Hou TY, Chu WY, Shen PC, Chen YY, Tan CJ, Hu JC, Chiu CC (2015) Geometrical effects of phospholipid olefinic bonds on the structure and dynamics of membranes: A molecular dynamics study. Biochim Biophys Acta 1848:1234–1247

Tsuchiya H (2015) Membrane interactions of phytochemicals as their molecular mechanism applicable to the discovery of drug leads from plants. Molecules 20:18923–18966

Utsugi T, Schroit AJ, Connor J, Bucana CD, Fidler IJ (1991) Elevated expression of phosphatidylserine in the outer membrane leaflet of human tumor cells and recognition by activated human blood monocytes. Cancer Res 51:3062–3066

van Meer G, Voelker DR, Feigenson GW (2008) Membrane lipids: where they are and how they behave. Nat Rev Mol Cell Biol 9:112–124

Vanommeslaeghe K, Hatcher E, Acharya C, Kundu S, Zhong S, Shim J, Darian E, Guvench O, Lopes P, Vorobyov I, Mackerell AD Jr (2010) CHARMM general force field: a force field for drug-like molecules compatible with the CHARMM all-atom additive biological force fields. J Comput Chem 31:671–690

Villalain J (2019) Epigallocatechin-3-gallate location and interaction with late endosomal and plasma membrane model membranes by molecular dynamics. J Biomol Struct Dyn 37:3122–3134

Wang Y, Markwick PR, de Oliveira CA, McCammon JA (2011) Enhanced lipid diffusion and mixing in accelerated molecular dynamics. J Chem Theory Comput 7:3199–3207

Wang XY, Zhang XH, Peng L, Liu Z, Yang YX, He ZX, Dang HW, Zhou SF (2017) Bardoxolone methyl (CDDO-Me or RTA402) induces cell cycle arrest, apoptosis and autophagy via PI3K/Akt/mTOR and p38 MAPK/Erk1/2 signaling pathways in K562 cells. Am J Transl Res 9:4652–4672

Wang YY, Zhe H, Zhao R (2014) Preclinical evidences toward the use of triterpenoid CDDO-Me for solid cancer prevention and treatment. Mol Cancer 13:30

Wu EL, Cheng X, Jo S, Rui H, Song KC, Davila-Contreras EM, Qi Y, Lee J, Monje-Galvan V, Venable RM, Klauda JB, Im W (2014) CHARMM-GUI Membrane Builder toward realistic biological membrane simulations. J Comput Chem 35:1997–2004

Yore MM, Kettenbach AN, Sporn MB, Gerber SA, Liby KT (2011) Proteomic analysis shows synthetic oleanane triterpenoid binds to mTOR. PLoS ONE 6:e22862

Zalba S, Ten Hagen TL (2017) Cell membrane modulation as adjuvant in cancer therapy. Cancer Treat Rev 52:48–57

Publisher's Note Springer Nature remains neutral with regard to jurisdictional claims in published maps and institutional affiliations.